

MODEL OF PIEZOELECTRIC POWER HARVESTING BEAM

Henry A. Sodano^a, Gyuhae Park^b, Donald J. Leo^a and Daniel J. Inman^a

^aCenter for Intelligent Material Systems and Structures
Virginia Polytechnic Institute and State University
Blacksburg, VA 24061-0261, USA

^bEngineering Sciences & Applications Division
Los Alamos National Laboratories
Los Alamos, New Mexico 87545

ABSTRACT

Piezoelectric materials can be used as mechanisms to transfer mechanical energy, usually ambient vibration into electrical energy that can be stored and used to power other devices. With the recent advances in wireless and MEMS technology, sensors can be placed almost anywhere necessary. Since these devices are wireless it becomes necessary that they have their own power supply. This power supply in most cases is the conventional battery, however problems can occur when using batteries because of their finite life span. When the battery is extinguished of all its power, the sensor must be retrieved and the battery changed. Because wireless sensors are developed so that they can be placed in remote locations such as structural sensors on a bridge or GPS tracking devices on animals in the wild, obtaining the sensor simply to replace the battery can become a very expensive task. Therefore, if a method of obtaining the untapped energy surrounding these sensors was implemented, significant life could be added to the power supply. One method is to use piezoelectric materials to obtain energy lost due to vibrations of the test specimen. This captured energy could then be used to prolong the life of the power supply or in the ideal case provide endless energy for the sensors lifespan. The goal of this study is to develop a model of the piezoelectric power harvesting device. This model would simplify the design procedure necessary for determining the appropriate size and vibration levels necessary for sufficient energy to be produced and supplied to the electronic devices. An experimental verification of the model is also performed to ensure its accuracy.

Keywords: Piezoelectric, power harvesting, wireless sensors

INTRODUCTION

Piezoelectric materials form transducers that are able to interchange electrical energy and mechanical strain or force. These materials, therefore, can be used as mechanisms to transfer ambient motion (usually vibration) into electrical energy that may be stored and used to power other devices. By implementing power harvesting devices, portable systems can be developed that do not depend on traditional methods for providing power, such as the battery, which has a limited operating life.

Recent studies, experiments and patents, indicate the feasibility of using PZT devices as power sources. Umeda, et al¹ uses a free-falling ball to impact a plate with a piezoceramic wafer attached to its underside, and developed an electrical equivalent model of the PZT transforming mechanical impact energy to electrical power. They also investigated the energy storage characteristics of the PZT with a bridge rectifier and a capacitor. Starner² examines the energy available from leg motion of a human being and surveys other human motion sources of mechanical energy including blood pressure. The author claims 8.4 watts of useable power can be achieved from a PZT mounted in a shoe. Kymissis et al³ examines using a piezofilm in addition to the ceramic used in reference 2, to provide power to light a bulb in a shoe, entirely from walking motion. Kimura's US Patent⁴ centers on the vibration of a small plate, harnessed to provide a rectified voltage signal. The

effort seems to be motivated by providing enough energy to run a small transmitter fixed to migratory birds for the purpose of transmitting their identification code and location. This result is also compared to using existing battery technology. Goldfarb et al⁵ presented a linearized model of a PZT stack and analyzed the efficiency of it as a power generation device. It was shown that the maximum efficiency occurs in a low frequency region much lower than the structural resonance of the stack. The efficiency is also related to the amplitude of the input force due to hysteresis of the PZT. In addition to the force applied in the poling direction (d_{33} mode), Clark and Ramsay⁶ have investigated and compared it with the transverse force (d_{31} mode) for a PZT generator. Their work showed that the d_{31} mode has a mechanical advantage in converting applied pressure to working stress for power generation. They concluded that a 1-cm² piezoceramic wafer can power a MEMS device in the microwatt range. Elvin et al⁷ theoretically and experimentally investigate the use of the self-powered strain energy sensors using PVDF. Their half-rectified circuit was then combined with a wireless communication device for human bone strain monitoring⁸. Kasyap et al⁹ formulated a lumped element model to represent the dynamic behavior of PZT in multiple energy domains using an equivalent circuit. Their model has been experimentally verified using a 1-d beam structure with the peak power efficiencies of approximately 20%. Gonzalez et al¹⁰ analyzed the prospect of piezoelectric based energy conversion, and suggested several issues to raise the electrical output power of the existing prototypes to the level that can be theoretically obtained. Ottman et al¹¹ investigated the effects of utilizing a DC-DC converter with an adaptive control algorithm to maximize power output of the piezoelectric element. Their efforts found that when using the adaptive circuit, energy was harvested at over for times the rate of direct charging without a converter.

It has been found that a piezoelectric device attached to a beam with cantilever boundary conditions provides an effective method of capturing transverse vibrations and converting them into useful electrical power. This configuration has proven itself to be effective in several previous experiments here at the Center for Intelligent Materials Systems and Structure (CIMSS), including recharging batteries¹² and other investigations into the amount of power capable of being produced through piezoelectric energy generation. This study concentrates on developing a model of a beam with piezoelectric elements attached that will provide an accurate estimate of the power generated through the piezoelectric effect. The model detailed in this paper is based off of a more general one developed by Hagood et al¹³ to estimate the performance of piezoelectric shunt damping circuits for active control. In addition, the model from Crawley et al¹⁴ was used to develop the actuation equations for piezoelectric devices and the constitutive equations of bimorphs were obtained from Smits et al¹⁵. An important addition to accommodate power harvesting that has been made to previous models, was to add

damping, which if not included causes the model to predict significantly more energy generation than actually developed in the real system. The results of our model will be presented in this paper as well as an experimental validation of the model.

NOMENCLATURE

α	= proportional damping constant
a	= acceleration
A	= amplitude of vibration
β	= proportional damping constant
b	= width of beam
c	= modulus of elasticity
C_p	= capacitance of piezoelectric
C	= damping matrix
δ	= variation
d_{ij}	= piezoelectric constant relating voltage and stress
D	= Electric Displacement
E	= electric field
e	= piezoelectric coupling coefficient
f	= external force
K	= stiffness
L	= length of beam
M	= mass
ϕ	= location of electrical potential
q	= electrical charge
ρ	= density
r	= temporal coordinate of displacement
R	= resistance
ϵ	= dielectric constant
S	= strain
t	= thickness of beam or time
t_p	= thickness of piezoelectric
T	= kinetic energy or stress in piezoelectric constitutive equations
θ	= piezoelectric coupling matrix
u	= displacement
U	= potential energy
v	= voltage
V	= volume
V.I.	= variational indicator
Φ	= mode shapes
ω	= natural frequency
ζ	= damping ratio

Superscript

E	= parameter at constant electrical field (short circuit)
S	= Value taken at constant strain
T	= parameter at constant stress or transpose

Subscript

p	= piezoelectric
s	= structure

MODEL OF PIEZOELECTRIC AND BEAM

The following derivation will use energy methods to develop the constitutive equations of a bimorph piezoelectric cantilever beam for power harvesting. To begin the derivation we will start with the general form of Hamilton's Principle. This states that the variational indicator must be zero at all time, as shown below in equation 4.1:

$$\text{V.I.} = \int_{t_1}^{t_2} [\delta T - \delta U + f\delta x] dt = 0 \quad (1)$$

The T , U and $f\delta x$ terms are defined by:

$$U = \frac{1}{2} \int_{V_s} \underline{S}^T \underline{T} dV_s + \frac{1}{2} \int_{V_p} \underline{S}^T \underline{T} dV_p - \int_{V_p} \underline{E}^T \underline{D} dV_p \quad (2)$$

$$T = \frac{1}{2} \int_{V_s} \rho_s \dot{\underline{u}}^T \dot{\underline{u}} dV_s + \frac{1}{2} \int_{V_p} \rho_p \dot{\underline{u}}^T \dot{\underline{u}} dV_p \quad (3)$$

$$f\delta x = \sum_{i=1}^{nf} \delta \underline{u}(x_i) \cdot \underline{f}_i(x_i) - \sum_{j=1}^{nq} \delta v_j \cdot \underline{q}_j \quad (4)$$

where U is the potential energy, T is the kinetic energy, $f\delta x$ is the external work applied to the system, S is the strain, T is the stress, E is the electric field, D is the electric displacement, V is the volume, u is the displacement, x is the position along the beam, v is the applied voltage, q is the charge, ρ is the density f is the applied force and the subscripts p and s , represent the piezoelectric material and the substrate, respectively. Before the variational indicator can be used to solve for the equations of motion the piezoelectric constitutive equations need to be introduced into the potential energy term and the variation of both the potential and kinetic energy must be found. First the piezoelectric constitutive equations will be introduced, which are:

$$\begin{bmatrix} \underline{T} \\ \underline{D} \end{bmatrix} = \begin{bmatrix} c^E & -e^T \\ e & \varepsilon^S \end{bmatrix} \begin{bmatrix} \underline{S} \\ \underline{E} \end{bmatrix} \quad (5)$$

where c is the modulus of elasticity, ε is the dielectric constant and The superscript, $()^S$, signifies the parameter was measured at constant strain and the superscript, $()^E$, indicates the parameter was measured at constant electric field (short circuit). These constitutive equations relate the electrical and mechanical properties of the piezoelectric element. The specification of these relationships will allow electromechanical interaction to be included in the model. The term e is the piezoelectric coupling coefficient and relates the stress to the applied electric field. The piezoelectric coupling

coefficient can be written as shown in equation 4.6 in terms of the more commonly specified coupling coefficient d by:

$$e = d_{ij} c^E \quad (6)$$

where c is the d_{ij} is the piezoelectric coupling coefficient with the subscript i and j referring to the direction of the applied field and the poling, respectively. Now we can incorporate the piezoelectric properties in the potential energy function:

$$U = \frac{1}{2} \left[\int_{V_s} \underline{S}^T c_s \underline{S} dV_s + \int_{V_p} \underline{S}^T c^E \underline{S} dV_p - \int_{V_p} \underline{S}^T e^T \underline{E} dV_p - \int_{V_p} \underline{E}^T e \underline{S} dV_p - \int_{V_p} \underline{E}^T \varepsilon^S \underline{E} dV_p \right] \quad (7)$$

Taking the variation of the kinetic energy from equation 4.3, and the potential energy term containing the piezoelectric properties of equation 4.7, yields:

$$\delta U = \int_{V_s} \delta \underline{S}^T c_s \underline{S} dV_s + \int_{V_p} \delta \underline{S}^T c^E \underline{S} dV_p - \int_{V_p} \delta \underline{S}^T e^T \underline{E} dV_p - \int_{V_p} \delta \underline{E}^T e \underline{S} dV_p - \int_{V_p} \delta \underline{E}^T \varepsilon^S \underline{E} dV_p \quad (8)$$

$$\delta T = \int_{V_s} \rho_s \delta \dot{\underline{u}}^T \dot{\underline{u}} dV_s + \int_{V_p} \rho_p \delta \dot{\underline{u}}^T \dot{\underline{u}} dV_p \quad (9)$$

The variations found in equations 4.4, 4.8 and 4.9 can be substituted into equation 4.1 to obtain the variational indicator:

$$\text{V.I.} = \int_{t_1}^{t_2} \left[\int_{V_s} \rho_s \delta \dot{\underline{u}}^T \dot{\underline{u}} dV_s + \int_{V_p} \rho_p \delta \dot{\underline{u}}^T \dot{\underline{u}} dV_p - \int_{V_s} \delta \underline{S}^T c_s \underline{S} dV_s - \int_{V_p} \delta \underline{S}^T c^E \underline{S} dV_p + \int_{V_p} \delta \underline{S}^T e^T \underline{E} dV_p + \int_{V_p} \delta \underline{E}^T e \underline{S} dV_p + \int_{V_p} \delta \underline{E}^T \varepsilon^S \underline{E} dV_p + \sum_{i=1}^{nf} \delta \underline{u}(x_i) \cdot \underline{f}_i(x_i) - \sum_{j=1}^{nq} \delta v_j \cdot \underline{q}_j \right] \quad (10)$$

This equation can now be used to solve for the equations of motion of any mechanical system containing piezoelectric elements. In order to solve equation 4.10 for the cantilever beam with bimorph piezoelectric elements some assumptions must be made. The first assumption follows the Rayleigh-Ritz procedure, which says that the displacement of the beam can be

written as the summation of modes in the beam and a temporal coordinate¹⁶:

$$u(x, t) = \sum_{i=1}^N \phi_i(x) r_i(t) = \underline{\phi}(x) \underline{r}(t) \quad (11)$$

where $\Phi_i(x)$ is the assumed mode shapes of the structure which can be set to satisfy any combination of boundary conditions, $r(t)$ is the temporal coordinate of the displacement and N is the number of modes to be included in the analysis. The second assumption made is to apply the Euler-Bernoulli beam theory. This allows the strain in the beam to be written as the product of the distance from the neutral axis and the second derivative of displacement with respect to the position along the beam. Once the strain is defined in this way equation 4.11 can be used to define the strain as follows:

$$\underline{S} = -y \frac{\partial^2 u(x, t)}{\partial x^2} = -y \underline{\phi}(x)'' r(t) \quad (13)$$

The third and last assumption is that the electric potential across the piezoelectric element is constant. This assumption also indicates that no field is applied to the beam, which in latter equations designates the beam to be inactive material:

$$\underline{E} = \psi(y) v(t) = \begin{cases} -v/t_p & t/2 < y < t/2 + t_p \\ 0 & -t/2 < y < t/2 \\ v/t_p & -t/2 - t_p < y < -t/2 \end{cases} \quad (14)$$

The previous assumption is for a beam with bimorph piezoelectric elements on the top and bottom of the beam as shown in Figure 4.1. The beam in Figure 4.1 also shows the notation for the geometry of the beam that is used throughout the derivation.

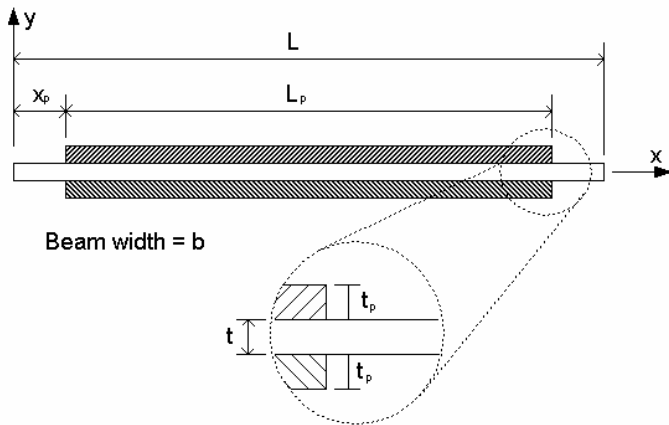


Figure 1. Schematic of a beam describing the variables.

Using the previous assumptions we can simplify the variational indicator to include terms that represent physical parameters. By doing this the equations describing the system become more recognizable when compared to those of a typical system and help give physical meaning to the parameters in the equations of motion. The mass matrices for the system can be written as:

$$M_s = \int_{V_s} \rho_s \underline{\phi}^T(x) \underline{\phi}(x) dV_s \quad (15)$$

$$M_p = \int_{V_p} \rho_p \underline{\phi}^T(x) \underline{\phi}(x) dV_p$$

The stiffness matrices can be written:

$$K_s = \int_{V_s} y^2 \underline{\phi}^T(x)'' c_s \underline{\phi}(x)'' dV_s \quad (16)$$

$$K_p = \int_{V_p} y^2 \underline{\phi}^T(x)'' c^E \underline{\phi}(x)'' dV_p$$

The electromechanical coupling matrix and the capacitance matrix are defined by:

$$\Theta = - \int_{V_p} y \underline{\phi}^T(x)'' e^T \psi(y) dV_p \quad (17)$$

$$C_p = \int_{V_p} \psi^T(y) \epsilon^S \psi(y) dV_p$$

The parameters defined in equations 4.15, 4.16 and 4.17 can be substituted into variational indicator of equation 4.10. This substitution allows the variational indicator to be written as:

$$\begin{aligned} \text{V.I.} = & \int_{t_1}^{t_2} \left[\delta \underline{r}^T(t) (M_s + M_p) \dot{\underline{r}}(t) - \delta \underline{r}^T(t) (K_s + K_p) \underline{r}(t) \right. \\ & + \delta \underline{r}^T(t) \Theta v(t) + \delta v(t) \Theta^T \underline{r}(t) + \delta v(t) C_p v(t) \\ & \left. + \sum_{i=1}^{nf} \delta \underline{r}(t) \phi(x_i)^T f_i(t) - \sum_{j=1}^{nq} \delta v q_j(t) \right] dt = 0 \end{aligned} \quad (18)$$

where $\delta()$ indicates the variation of the corresponding variable. Taking the integral of the variational indicator leaves two coupled equations. The two equations shown below are coupled by the previously defined electromechanical coupling matrix Θ . The top equation defines the mechanical motion and the bottom equation defines the electrical properties of the system:

$$(M_s + M_p)\ddot{r}(t) + (K_s + K_p)r(t) - \Theta v(t) = \sum_{i=1}^{nf} \phi(x_i)^T f_i(t) \quad (19)$$

$$\Theta^T r(t) + C_p v(t) = q(t)$$

These equations now represents the electro-mechanical system and can be used to determine the motion of the beam, however this system of equations does not contain any energy dissipation. Because the model is intended to represent a power harvesting system that must be removing energy, this form is not suitable for our needs, as it does not account for energy lost through the structure. In addition, the energy removed from the system through energy harvesting must be accounted for. To incorporate energy dissipation into the equation we can use ohm's law and add a resistive element between the positive and negative electrodes of the piezoelectric. The resistive element will provide a means of removing energy from the system. If we do this the electrical boundary condition becomes:

$$v_i(t) = -R\dot{q}(t) \quad (20)$$

In addition to this, the system should have some type of additional mechanical damping that needs to be accounted for. If only the electrical damping is accounted for the model will over predict the actual amount of power generated. The amount of mechanical damping added to the model was determined from experimental results. This is done using proportional damping methods and the damping ratio that is predicted from the measured frequency response function. With the damping ratio known, proportional damping can be found from¹⁶:

$$C = \alpha(M_s + M_p) + \beta(K_s + K_p) \quad (21)$$

where α and β are determined from:

$$\zeta_i = \frac{\alpha}{2\omega_i} + \frac{\beta\omega_i}{2} \quad i = 1, 2, \dots, n \quad (22)$$

where ζ_i is the damping ratio found from the frequency response of the structure. Incorporating equations 4.20 and 4.21 into equation 4.19, results in the final model of the power harvesting system:

$$(M_s + M_p)\ddot{r}(t) + C\dot{r}(t) + (K_s + K_p)r(t) - \Theta v(t) = \sum_{i=1}^{nf} \phi(x_i)^T f_i(t) \quad (23)$$

$$R\dot{q}(t) - C_p^{-1}\Theta^T r(t) + C_p^{-1}q(t) = 0$$

Equation 4.23 shown above provides an accurate model of the power harvesting system. The $\dot{q}(t)$ term provides the current output of the piezoelectric element and can be directly related to the power output of the piezoelectric through the load resistance R .

The last portion of our model left undefined is the forcing function. The system that we are investigating as mentioned earlier is a cantilever beam that is excited by transverse vibrations of the structure that it is clamped to; therefore no force is directly applied to the beam. Instead the clamped end of the beam is experiencing base motion and transferring that energy to the beam through it own inertia. The standard boundary conditions of the clamped end of the beam indicate that the slope and displacement are zero at all time. In the case of base motion, the zero displacement condition would not be held and a new set of mode shapes would need to be generated. Rather than doing this, it was decided that a force corresponding to the inertia of the beam when subjected to the base motion could be used and the clamped-free mode shapes would still hold valid. The forcing function used to model the inertia of the beam is shown below in equation 24.

$$f(t) = \int_0^L \int_0^b \int_0^t \rho A \omega^2 \sin(\omega t) dz dy dx \quad (24)$$

With the forcing function defined everything necessary to simulate the power harvesting system is included in the model. The following sections of this paper will describe the experimental procedures and results, in order to show the accuracy of this model.

EXPERIMENTAL SETUP

The accuracy of the model was tested on a Midé Technology Corporation Quick Pack model QP40N, although it could be used to model any beam with a piezoelectric element attached. The QP40N is a bimorph actuator with dimensions and properties shown in Figure 2. The Quick Pack is a piezoelectric actuator that is constructed from four piezo wafers embedding in a Kapton and epoxy matrix. The experiments were performed to test the amount of power generated from this device when subjected to transverse vibrations of varying frequency and amplitude. As mentioned previously, we were interested in the quick Pack being mounted with cantilever boundary conditions. To provide the transverse vibration the Quick Pack actuator was mounted to an electromagnetic shaker as shown in Figure 3.



Device size (mm): 100.6 x 25.4 x 0.762
 Device weight (g): 9.52
 Piezo wafer size (mm): 45.974 x 20.574 x 0.254

Figure 2. Midé Technology Corporation Quick Pak model QP40N (Figure from Midé Technology Corporation).

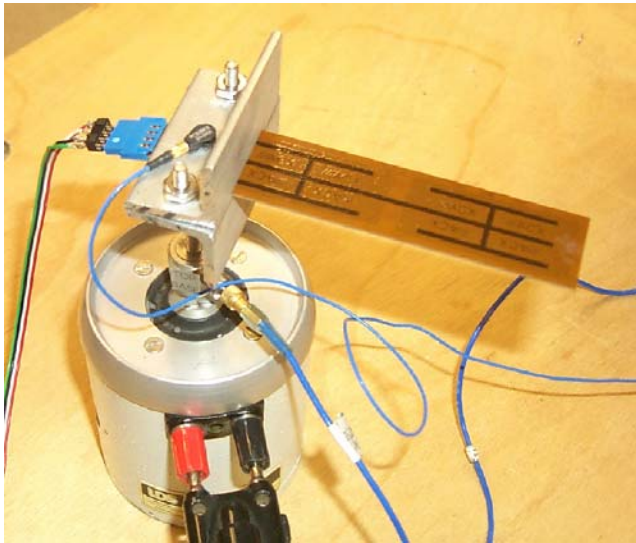
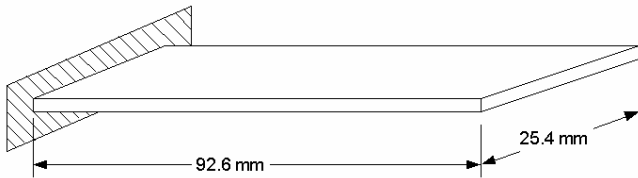


Figure 3. Quick Pack QP40N attached to the shaker and dimensions of beam when one end is clamped.

One complication that arose when modeling the Quick Pack actuator was due to its composite structure and the piezoelectric wafers not spanning the entire length of the beam, which can be seen in Figure 2. Because the area of the beam with no piezoelectric wafer consisted of only Kapton and epoxy, it contained a localized lower modulus of elasticity. Midé Technology Corporation could not supply a value for the effective modulus of the complete beam. Therefore, the setup shown in Figure 4 was constructed to measure the stiffness of the Quick Pack. To obtain a value for the stiffness we needed to measure the force applied to the beam and its corresponding displacement. The experimental setup to do this consisted of a Transducer Techniques 100 gram load cell, model GSO-100C

and a polytec laser vibrometer. The load cell was mounted on a lead screw to allow a steady force to be applied at the tip of the beam. The result of this test found the modulus of the beam to be 2.5 GPa. The reason for this value being so low is due to the area at the mid-span of the beam that consisted of only the Kapton and epoxy. When the static tests were performed on the beam it was apparent that the majority of the bending was occurring at this location. Therefore, it was concluded that the experimental tests performed had actually measured the modulus of elasticity corresponding to the Kapton and epoxy portion of the beam. This still left the overall modulus of the beam unknown. To calculate the modulus for the beam we simply averaged the modulus of the piezoelectric material, that was supplied by Midé and the experimentally found modulus for the Kapton and epoxy matrix according to their individual percent of the cross sectional area. The resulting modulus of elasticity and the other piezoelectric properties used are shown in Table 1.

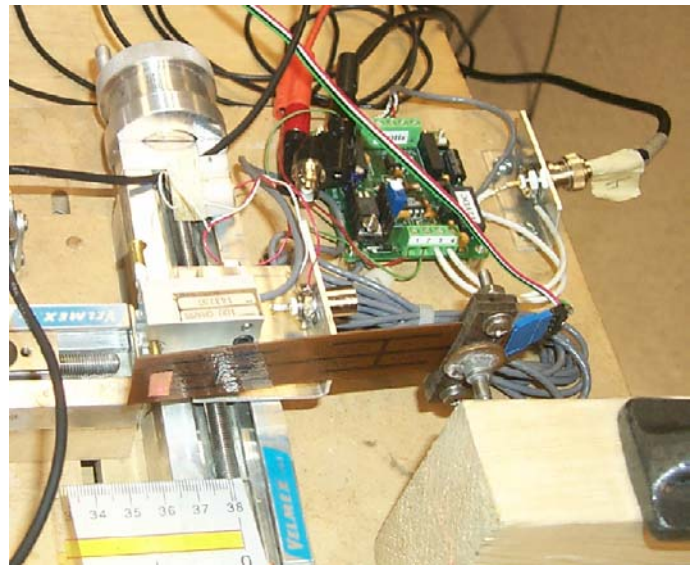


Figure 4. Experimental setup used to find the elastic modulus of the Kapton-epoxy matrix.

Table 1. Properties of the Quick Pack

Property	Symbol	Value
Dielectric Constant	k_3^T	1800
Piezoelectric Strain Coefficient	d_{13}	-179×10^{-12} m/volt
Modulus of Piezoelectric	c^E	63 GPa
Modulus of Kapton-epoxy	c_s	2.5 GPa
Modulus of Quick Pack	c_b	35.17 GPa
Density of Piezo Material	ρ	7700 kg/m ³
Density Composite Matrix	ρ	2150 kg/m ³

MODEL VERIFICATION

The accuracy of the model was compared against experimental results to show that it can accurately predict the amount of power produced by the Quick Pack when subjected to transverse vibration. To ensure that the model and experimental tests were similar an accelerometer was used to calculate the amplitude of the sinusoidal force applied to the beam through:

$$a = A\omega^2 \sin(\omega t) \Rightarrow A_{\max} = \frac{a}{\omega^2} \quad (25)$$

where a is the acceleration of the clamped end of the beam. The beam was excited by a sinusoidal input and the steady state power output was measured across several different resistors. The frequency response of the model and the experimentally tested Quick Pack is shown in Figure 5. The differences in the two responses are attributed to the Quick Pack's composite structure resulting in coupled modes and the nonlinear properties of the Kapton material, especially its modulus of elasticity that varies nonlinearly with frequency. It is expected that a beam constructed of a homogeneous material with a piezoelectric mounted to its surface would produce a more accurate frequency response.

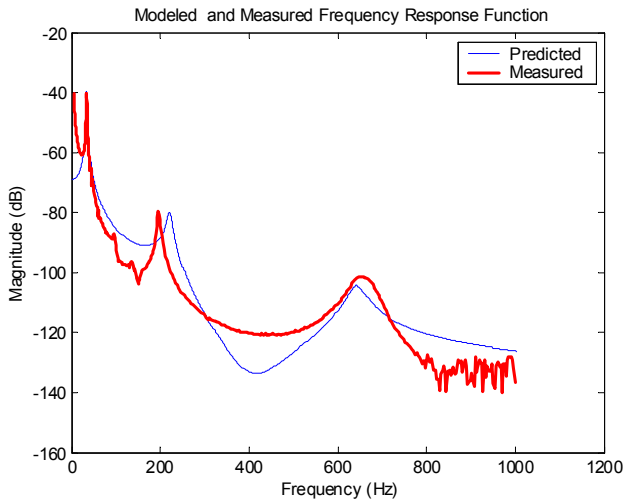


Figure 5. Frequency response of the model and the experimental data.

The output current of the Quick Pack was compared to the output current of the model for various frequencies. The output current across a 10kΩ resistor for several frequencies of the model and that obtained through experiments are shown in Figure 6. Figures 7 and 8, show the output current across a 100Ω and 100kΩ resistor for various frequencies. These figures show that the model is very accurate for providing the power generated at various frequencies and resistive loads.

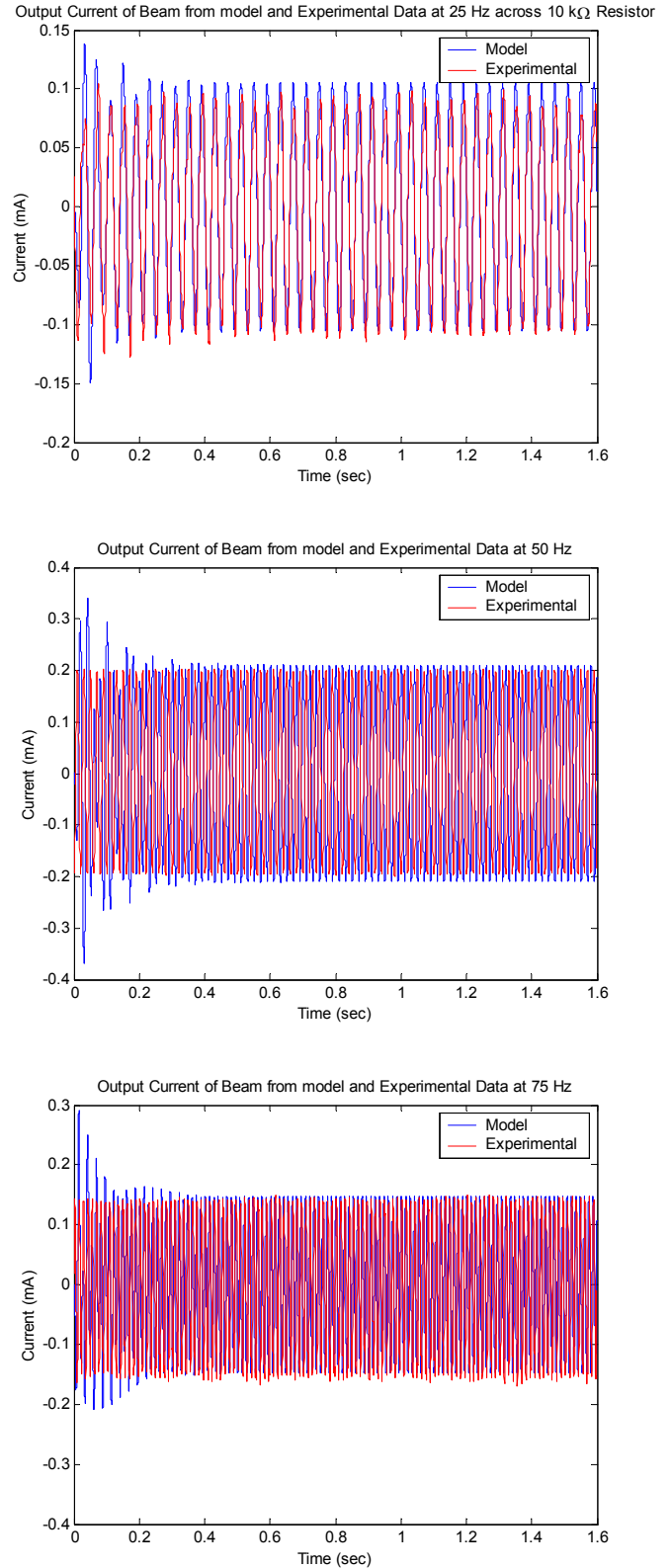


Figure 6. Output current across a 10kΩ resistor of the model and the experiment for 25Hz, 50Hz and 75Hz, respectively.

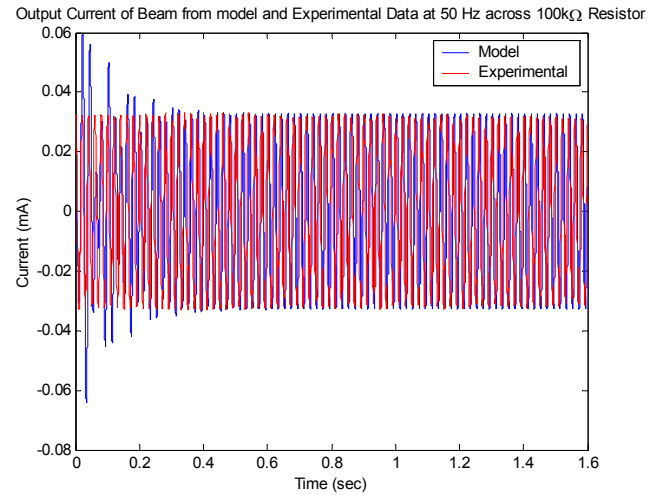
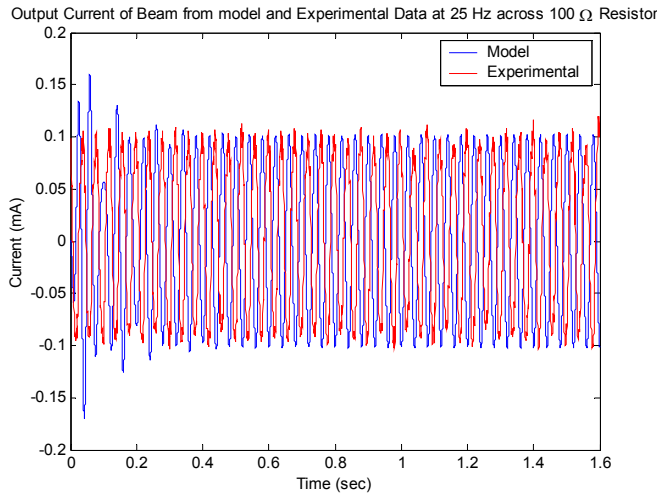


Figure 7. Output current across a 100Ω of the model and the experiment for 25Hz and 50Hz, respectively.

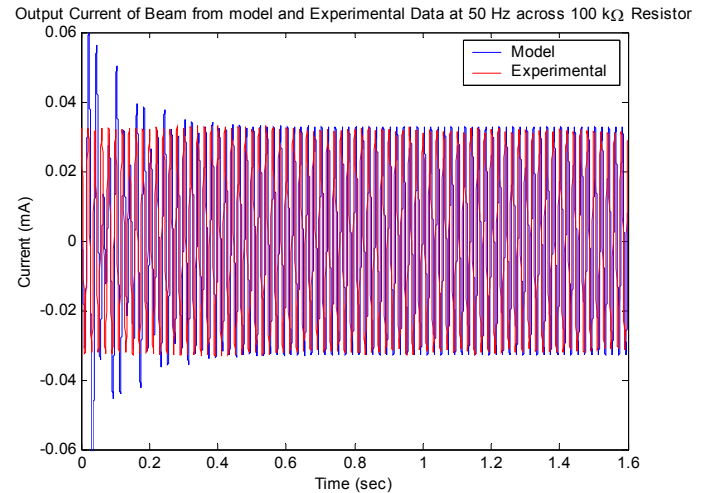
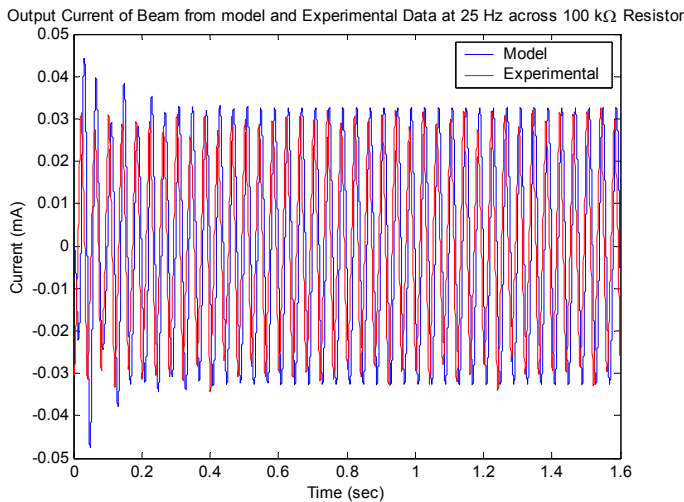


Figure 8. Output current across a $100k\Omega$ resistor of the model and the experiment for 25Hz and 50Hz, respectively.

In addition to providing an accurate estimate of the of the power generated by a beam with complicated piezoelectric layout and a non-homogeneous material composition, the model also shows that power harvesting works much like a shunt damper. In the presences of a power harvesting circuit energy is taken for the system and supplied to the electrical components causing a damping effect. This effect is very similar to one of the original uses of the model developed in Hagood et al,¹³ which was used to show the ability of a tuned RLC circuit to effectively damp the vibration in a beam. The major difference is that in our case we are working with a load resistance which will also induce damping to the system but over a broad range of frequencies rather than the turned

frequency of a RLC circuit. The damping effects of power harvesting on an impulse response with three different load resistances are shown in Figures 9, 10 and 11. It is apparent that as more energy is removed from the system the impulse dies out faster until a critical level where the resistive load of the circuit exceeds the impedance of the piezoelectric network causing lower efficiency power generation. Therefore, power harvesting works in much the same way as shunt damping, but the energy is then stored for use instead of dissipating it.

CONCLUSIONS

A model was developed to predict the amount of power capable of being generated through the vibration of a cantilever beam with piezoelectric elements. The model was compared to

experimental results and shown to be very accurate independent of excitation frequency and load resistance. In addition, the model was applied to a structure the contained complex piezoelectric layout and a non-homogenous material beam, indicating that the model is robust and can be applied to a variety of different mechanical conditions. The damping effects of power harvesting were also shown to be predicted in the model and to follow that of a resistive shunt damping circuit. This model provides a design tool for developing power harvesting systems by assisting in determining the size and level of vibration needed to produce the desired level of power generation. The potential benefits of power harvesting and the advances in low power electronics and wireless sensors are making the future of this technology look very bright. Future work in modeling of the power harvesting system consists of developing a similar model for a piezoelectric applied to a plate.

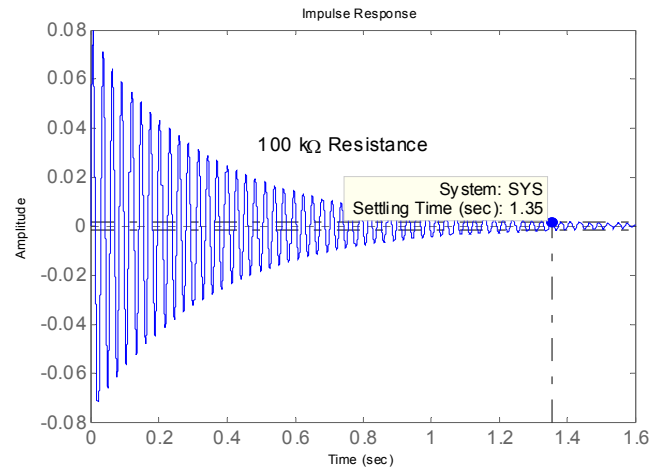


Figure 11. Impulse Response with a 100kΩ Resistive Load.

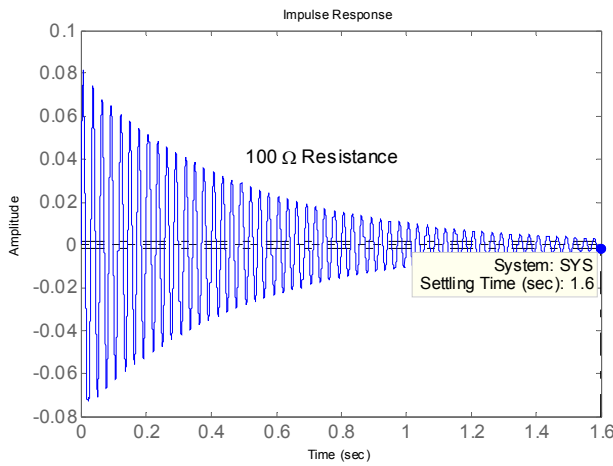


Figure 9. Impulse response with a 100Ω resistive load.

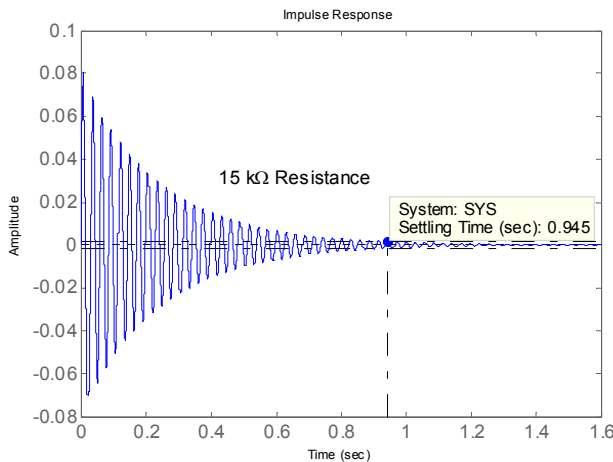


Figure 10. Impulse Response with a 15kΩ Resistive Load.

ACKNOWLEDGMENTS

This work was sponsored by The Goodson Professorship. The authors gratefully acknowledge the support.

REFERENCES

1. Umeda, M., Nakamura, K. and Ueha, S., 1996, "Analysis of the Transformation of Mechanical Impact Energy to Electrical Energy Using a Piezoelectric Vibrator", *Japanese Journal of Applied Physics*, Vol. 35, Part1, No. 5B, May, pp. 3267-3273.
2. Starner, T., 1996, "Human-Powered Wearable Computing," *IBM Systems Journal*, Vol. 35, pp. 618.
3. Kymissis, J., Kendall, C., Paradiso, J., Gershenfeld, N., 1998, "Parasitic Power Harvesting in Shoes," *Second IEEE International Conference on Wearable Computing*, pp. 132-139.
4. Kimura, M, 1998, "Piezoelectric Generation Device", US Patent Number 5,801,475.
5. Goldfarb, M. and Jones, L. D., 1999. "On the Efficiency of Electric Power Generation with Piezoelectric Ceramic," *Journal of Dynamic Systems, Measurement, and Control*, Vol. 121, pp 566-571.
6. Clark, W. and Ramsay, M. J., 2000. "Smart Material Transducers as Power Sources for MEMS Devices," *International Symposium on Smart Structures and Microsystems*, Hong Kong.

7. Elvin, N.G., Elvin, A.A., and Spector, M., 2001, "A self-Powered Mechanical Strain Energy Sensor," *Smart Materials and Structures*, Vol. 10, pp. 293-299.
8. Elvin, N.G., Elvin, A.A., and Spector, M., 2000, "Implantable bone strain telemetry system and method," US Patent Specification 6034296.
9. Kasyap, A., Lim, J., Johnson, D., Horowitz, S., Nishida, T., Ngo, K., Sheplak, M., Cattafesta, L., 2002. "Energy Reclamation from a Vibrating Piezoceramic Composite Beam," *Proceedings of 9th International Congress on Sound and Vibration*, Orlando, FL.
10. Gonzalez, J.L., Moll, F., Rubio, A. "A prospect on the use of Piezoelectric Effect to Supply Power to Wearable Electronic Devices," ICMR 2001, Akita, Japan, October 2001, pp. Vol1,202-207.
11. Ottman, G.K., Hofmann, H., Bhatt A. C., Lesieutre, G. A., 2002, "Adaptive Piezoelectric Energy Harvesting Circuit for Wireless, Remote Power Supply," *IEEE Transactions on Power Electronics*, Vol. 17, No.5.
12. Sodano, H.A., Park, G., Leo, D., Inman, D.J., 2003, "Use of Piezoelectric Energy Harvesting Devices for Charging Batteries," *Proceedings of SPIE's 10th Annual International Symposium on Smart Structures and Materials*, Vo. 5050.
13. Hagood, N.W., Chung, W.H., Von Flotow, A., 1990, "Modelling of piezoelectric Actuator Dynamics for Active Structural Control," *Journal of Intelligent Material Systems and Structures*, Vol. 1, no. 3, p. 327-354.
14. Crawley, E.F., Anderson, E.H., 1990, "Detailed Models of Piezoceramic Actuation of Beams," *Journal of Intelligent Material Systems and Structures*, Vol. 1, no. 1, p. 4-25.
15. Smits, J., Dalke, S., Cooney, T.K., 1991, "The Constituent Equations of Piezoelectric Bimorphs," *Sensors and Actuators*, Vol. 28, pp. 41-61.
16. Inman, D.J., 2001, *Engineering Vibration*, Prentice-Hall, Inc., Upper Saddle River, New Jersey.